



# LUND UNIVERSITY

## Linking the progressive expansion of reducing conditions to a stepwise mass extinction event in the late Silurian oceans

Bowman, Chelsie N.; Young, Seth A.; Kaljo, Dimitri; Eriksson, Mats E.; Them, Theodore R.; Hints, Olle; Martma, Tõnu; Owens, Jeremy D.

Published in:  
Geology

DOI:  
[10.1130/G46571.1](https://doi.org/10.1130/G46571.1)

2019

[Link to publication](#)

### Citation for published version (APA):

Bowman, C. N., Young, S. A., Kaljo, D., Eriksson, M. E., Them, T. R., Hints, O., Martma, T., & Owens, J. D. (2019). Linking the progressive expansion of reducing conditions to a stepwise mass extinction event in the late Silurian oceans. *Geology*, 47(10), 968-972. <https://doi.org/10.1130/G46571.1>

Total number of authors:  
8

### General rights

Unless other specific re-use rights are stated the following general rights apply:  
Copyright and moral rights for the publications made accessible in the public portal are retained by the authors and/or other copyright owners and it is a condition of accessing publications that users recognise and abide by the legal requirements associated with these rights.

- Users may download and print one copy of any publication from the public portal for the purpose of private study or research.
- You may not further distribute the material or use it for any profit-making activity or commercial gain
- You may freely distribute the URL identifying the publication in the public portal

Read more about Creative commons licenses: <https://creativecommons.org/licenses/>

### Take down policy

If you believe that this document breaches copyright please contact us providing details, and we will remove access to the work immediately and investigate your claim.

LUND UNIVERSITY

PO Box 117  
221 00 Lund  
+46 46-222 00 00

1 *"This is the peer reviewed version of the following article: Bowman et al. 2019:*  
2 *Linking the progressive expansion of reducing conditions to a stepwise mass extinction event in the*  
3 *late Silurian oceans. Geology 47, 968–972., which has been published in final form at*  
4 *<https://doi.org/10.1130/G46571.1>"*  
5  
6

7 **Linking the progressive expansion of reducing conditions to a stepwise mass extinction event in the**  
8 **late Silurian oceans**  
9

10 **Chelsie N. Bowman<sup>1</sup>, Seth A. Young<sup>1</sup>, Dimitri Kaljo<sup>2</sup>, Mats E. Eriksson<sup>3</sup>, Theodore R. Them II<sup>4</sup>,**  
11 **Olle Hints<sup>2</sup>, Tõnu Martma<sup>2</sup>, and Jeremy D. Owens<sup>1</sup>**

12 <sup>1</sup>*Department of Earth, Ocean and Atmospheric Science | National High Magnetic Field Laboratory,*  
13 *Florida State University, Tallahassee, FL, 32304, USA*

14 <sup>2</sup>*Department of Geology, Tallinn University of Technology, Ehitajate tee 5, 19086 Tallinn, Estonia*

15 <sup>3</sup>*Department of Geology, Lund University, Sölvegatan 12, SE-223 62 Lund, Sweden*

16 <sup>4</sup>*Department of Geology and Environmental Geosciences, College of Charleston, Charleston, SC, 29424,*  
17 *USA*  
18

19 **ABSTRACT**

20 The late Ludlow Lau Event was a severe biotic crisis in the Silurian, with resurgent microbial  
21 facies and faunal turnover rates otherwise only documented with the “big five” mass extinctions. This  
22 asynchronous late Silurian marine extinction event preceded an associated positive carbon isotope  
23 excursion, the Lau CIE, although a mechanism for this temporal offset remains poorly constrained. Here  
24 we report thallium isotope data from locally reducing late Ludlow strata within the Baltic Basin to  
25 document the earliest onset of global marine deoxygenation. The initial expansion of anoxia coincides  
26 with the onset of the extinction and therefore precedes the Lau CIE. Additionally, sulfur isotope data  
27 record a large positive excursion parallel to the Lau CIE, interpreted to indicate a major increase in pyrite  
28 burial associated with the widely documented carbon isotope excursion. This suggests a possible global  
29 expansion of euxinia (anoxic and sulfidic water-column) following deoxygenation. These data are the  
30 most direct proxy evidence of paleo-redox conditions that link the known extinction to the Lau CIE  
31 through the progressive expansion of anoxia, and most likely euxinia, across portions of the late Silurian  
32 oceans.  
33

34 **INTRODUCTION**

35 High rates of evolutionary turnover and severe, punctuated extinctions of marine taxa were a  
36 hallmark of the Silurian (e.g., Jeppsson, 1998; Crampton et al., 2016). This interval occurred during the  
37 transition from the Late Ordovician icehouse to Devonian greenhouse worlds when a dynamic ocean-  
38 atmosphere system oscillated between cool and warm conditions (e.g., Jeppsson, 1998). Recurrent  
39 extinctions in graptolites and conodonts were associated with the transitions between the alternating  
40 climate states, the most notable being the globally-documented late Ludlow Lau extinction (Jeppsson,  
41 1998; Calner, 2005; Crampton et al., 2016). This extinction was first recognized using conodonts from  
42 carbonate platform successions (termed the Lau event; e.g. Jeppsson and Aldridge, 2000) and then in  
43 graptolite studies of deeper-water shale sequences (termed the Kozlowskii event; Koren', 1993; Urbanek,  
44 1993), herein referred to as the Lau/Kozlowskii extinction (LKE). The LKE is at least the tenth largest  
45 extinction event in Earth history with ~ 23% loss of genera (e.g., Bond and Grasby, 2017 and references  
46 therein). In addition to conodonts and graptolites, it affected a wide range of marine taxa including  
47 brachiopods (Talent et al., 1993), fishes (Eriksson et al., 2009), and acritarchs (Stricanne et al., 2006).  
48 Extinctions of individual taxonomic groups are asynchronous, with documented extinctions in benthic  
49 and nektonic groups preceding the planktic organisms (e.g., Munnecke et al., 2003; Stricanne et al., 2006;  
50 Calner, 2008). The LKE shares similar characteristics to the “big five” mass extinctions such as the

51 survival of disaster fauna and a resurgence of microbially-mediated sedimentary facies (e.g., Talent et al.,  
52 1993; Jeppsson, 2005; Calner, 2005, 2008; Eriksson et al., 2009).

53 Despite the magnitude and complexity of the LKE, its mechanistic underpinnings are not well-  
54 constrained. An expansion of reducing conditions has been implicated as a potential driver of the  
55 observed temporal-stepwise extinction (e.g. Munnecke et al., 2003; Stricanne et al., 2006). This  
56 hypothesis is also used to explain the possibility of extensive burial of organic carbon, resulting in the  
57 Lau positive carbon isotope excursion (CIE; e.g. Saltzman, 2005), but this cannot explain the temporal  
58 offset between the LKE and the Lau CIE. Further, organic carbon burial can be affected by other factors  
59 (e.g., Canfield, 1994). Variations in eustatic sea level and carbonate weathering rates have also been  
60 invoked as a potential mechanism for driving positive CIEs (e.g., Hirnantian CIE; Kump et al., 1999).  
61 However, a global expansion of reducing conditions provides a kill mechanism and can be tested using  
62 combined traditional and novel paleo-redox proxies.

63 This study investigates the relationship between the LKE and Lau CIE in the context of changing  
64 marine redox conditions in upper Silurian (Ludfordian Stage) strata from the Baltic Basin. In order to  
65 reconstruct the evolution of global marine redox conditions we measured thallium (Tl) isotopes,  
66 manganese (Mn) concentrations, and pyrite sulfur isotopes ( $\delta^{34}\text{S}_{\text{pyr}}$ ) from a distal shelf/slope setting  
67 (Latvia) and carbonate-associated sulfate (CAS) sulfur isotopes ( $\delta^{34}\text{S}_{\text{CAS}}$ ) from a shallow shelf setting  
68 (Gotland, Sweden; Fig. 1). This multi-proxy, multi-lithology approach aims to establish a first-order link  
69 between the fossil record of stepwise extinction, carbon burial, and the progression from more oxygenated  
70 to more reducing conditions in the late Silurian seas.

## 71 72 **GEOLOGIC SETTING**

73 The Baltic Basin was located in a tropical, epicratonic seaway on the southern margin of the  
74 paleocontinent Baltica (e.g., Eriksson and Calner, 2008; Fig. 1; Fig. DR1). In the late Silurian, the  
75 northern and eastern edges of the basin were delineated by rimmed carbonate shelves with parallel facies  
76 belts ranging from lagoonal deposits in the north to deep-shelf shales and marls in the south, deepening  
77 towards the Rheic Ocean (Eriksson and Calner, 2008). The Uddvide-1 drill core and nearby outcrops on  
78 the island of Gotland, Sweden are predominantly carbonates from the shallow shelf area of the basin (for  
79 more details see Eriksson and Calner, 2008). The Priekule-20 drill core from southwestern Latvia is  
80 predominantly shales and marls from a correlative deep shelf setting (details in Kaljo et al., 1997).

## 81 82 **METHODS AND RESULTS**

83 Two study localities were analyzed for  $\delta^{13}\text{C}$  records, organic or inorganic (micrite), to investigate  
84 carbon cycle dynamics. Pyrite sulfur was extracted from shale samples using a widely accepted chromium  
85 reduction method, and CAS was extracted from carbonates following standard methods. Full details of all  
86 analytical methods are given in the GSA Data Repository<sup>1</sup>. Sulfur isotopes were analyzed to investigate  
87 global pyrite burial ( $\delta^{34}\text{S}_{\text{CAS}}$ ) and the potential imprints on local signatures ( $\delta^{34}\text{S}_{\text{pyr}}$ ). Sedimentary Tl  
88 isotopes ( $\epsilon^{205}\text{Tl} = [(R_{\text{sample}}/R_{\text{reference}}) - 1] \times 10^4$ ) have been used to investigate the earliest onset of global  
89 marine deoxygenation during Mesozoic CIEs (Ostrander et al., 2017; Them et al., 2018). During Mn-  
90 oxide precipitation, Tl is adsorbed with a large positive isotope fractionation, thus leaving seawater  
91 isotopically lighter (as reviewed in Nielsen et al., 2017). Precipitation and burial of Mn-oxides require  
92 oxic bottom-water conditions, the expanse of which represents the dominant seawater control of Tl-  
93 isotope composition on time scales  $< \sim 5$  million years (Nielsen et al., 2017; Owens et al., 2017). The  
94 global seawater Tl-isotope signal is recorded in euxinic marine settings and in anoxic waters with sulfide  
95 near the sediment-water interface from basins that are well-connected to the open ocean (Owens et al.,  
96 2017). Consequently, reconstructing the Tl isotope composition of late Silurian seawater provides  
97 evidence for initial changes in global marine oxygenation by tracking the burial flux of Mn-oxides  
98 relative to the extinction, CIE, and additional redox proxies (e.g., Ostrander et al., 2017; Them et al.,  
99 2018). Importantly, a large Tl isotope fractionation is not associated with the burial of other Mn-bearing  
100 minerals (e.g., sulfides, carbonates). Constraining locally reducing conditions using an independent  
101 geochemical proxy is necessary to interpret Tl isotopes as a temporal seawater signature and to avoid

102 contamination via local Mn-oxides (Owens et al., 2017). Low total Mn concentrations [Mn] are indicative  
103 of locally reducing conditions (e.g. Boyer et al., 2011) and, thus, utilized in this study.

104 The Lau CIE is documented in  $\delta^{13}\text{C}_{\text{carb}}$  and  $\delta^{13}\text{C}_{\text{org}}$  records from the outer shelf setting (Fig. 2A),  
105 with values increasing within the upper part of the *Bohemograptus bohemicus tenuis*-*Neocucullograptus*  
106 *kozlowskii* zones, reaching peak values of +5.7‰ and -23.5‰, respectively, in the Nova Beds of the  
107 Dubysa Formation (Fm). The  $\delta^{13}\text{C}$  records return to baseline values in the overlying Engure Fm. There is  
108 a positive ~40‰ excursion in  $\delta^{34}\text{S}_{\text{pyr}}$  data (baseline values ~-22‰ shift to peak values of up to ~+15‰)  
109 that coincides with the Lau CIE within the upper Nova Beds and basal Engure (Fig. 2B). [Mn] are low  
110 throughout the section with average values of 363 and 552 ppm in the lower to middle Dubysa and  
111 Engure, respectively (Fig. 2C). The  $\epsilon^{205}\text{Tl}$  record shows baseline values in the lower to middle Dubysa of  
112 -4.1 to -4.6 (Fig. 2D). This is followed by a positive excursion in  $\epsilon^{205}\text{Tl}$  values that peaks at -2.6 and  
113 averages -3.3 throughout the rest of the drill core.

114 The Lau CIE is also documented in both  $\delta^{13}\text{C}_{\text{carb}}$  and  $\delta^{13}\text{C}_{\text{org}}$  records from the inner shelf  
115 carbonates (Fig. 3A), with values beginning to rise in the upper När Fm and peaking in the overlying Eke  
116 Fm (*Icriodontid* Zone) at +7.5‰ and -24.0‰. Within the Burgsvik Sandstone,  $\delta^{13}\text{C}_{\text{carb}}$  values decline to  
117 ~+4.0‰, while  $\delta^{13}\text{C}_{\text{org}}$  values increase to -22.9‰, which is followed by a return to peak  $\delta^{13}\text{C}_{\text{carb}}$  values of  
118 +7.5‰ in the overlying Burgsvik Oolite (*Ozarkodina snajdri* Zone). The overlying Hamra Fm and  
119 Sundre Fm record the falling limb of the CIE, but not post-excursion baseline values. There is a positive  
120 ~30‰ excursion in the  $\delta^{34}\text{S}_{\text{CAS}}$  record (Fig. 3B), with initial values ~+11‰ in the När that rise through  
121 the Eke to values of ~+22‰. The  $\delta^{34}\text{S}_{\text{CAS}}$  values then continue rising through Burgsvik Oolite, Hamra,  
122 and Sundre to +40.6‰.

## 123 124 **DISCUSSION**

125 The [Mn] from the Latvia deep shelf setting (Fig. 2C) are all below the average crustal values and  
126 suggest depleted local Mn deposition, and therefore locally reducing conditions throughout the studied  
127 interval (Boyer et al., 2011). Cross-plotting [Mn] and Tl isotopes shows no significant correlation (Fig.  
128 DR2I). Thus, it is unlikely that local Mn-oxide burial has influenced the Tl-isotope seawater signature.  
129 The observed positive shift in Tl isotopes from ~-4.6 to -2.6 begins within the Ludfordian *B. bohemicus*  
130 *tenuis* graptolite biozone (Fig. 2D) and signifies a decline in the global burial of Mn-oxides. The  
131 reduction in Mn-oxide burial is likely due to significant bottom-water deoxygenation as anaerobic  
132 microbial metabolisms kept pace with carbon export, reducing bottom water oxidants such as oxygen and  
133 Mn-oxides, but not yet reducing enough to increase widespread organic carbon preservation and burial  
134 (e.g., Ostrander et al., 2017; Them et al., 2018). This early onset of deoxygenation coincides with the  
135 initial phase of extinction (e.g., brachiopods, fish, and conodonts) that predates the Lau CIE (Fig. 4; e.g.  
136 Calner, 2008). Extinctions in these nektonic and benthic taxa coincide with the rising limb of the positive  
137 Tl-isotope excursion, which begins ~ 8 m before the Lau CIE. This suggests that deoxygenation and  
138 subsequent spread of anoxia was responsible for the initial phases of extinction in fauna living at/near the  
139 sediment-water interface and within deeper waters ~175 to 270 kyr prior to the Lau CIE (see GSA Data  
140 Repository for calculations). For the first time in the Paleozoic, this stratigraphic relationship of  
141 extinction/turnover, and C- and Tl-isotopes is observed. A similar progression of events has been  
142 suggested for two Mesozoic oceanic anoxic events or OAEs (Ostrander et al., 2017; Them et al., 2018),  
143 but with varying magnitudes and durations.

144 The positive C- and S-isotope excursions (Figs. 2 and 3) are consistent with transient increases in  
145 the amount of reduced C and S buried globally as organic matter, pyrite, and possibly organic sulfur  
146 compounds (e.g., Gill et al., 2011; Owens et al., 2013; Raven et al., 2019). Sea level may also have been a  
147 contributing, but secondary, factor to the Lau CIE (see GSA Data Repository for further discussion). This  
148 suggests the Lau CIE began as export and burial of organic carbon to the seafloor outpaced consumption  
149 via remineralization, which was likely dependent on a sufficiently large portion of shelf and other marine  
150 environments being affected by deoxygenation and expansion of anoxia. The excess organic matter  
151 available fueled microbial sulfate reduction (MSR) and ultimately increased pyrite burial as MSR-

152 produced H<sub>2</sub>S reacted with reactive iron minerals in sulfidic environments. The burial fractions of  
153 reduced C and S were preferentially enriched in <sup>12</sup>C and <sup>32</sup>S due to fractionations associated with  
154 biological processes, and the remaining seawater was enriched in <sup>13</sup>C and <sup>34</sup>S. Euxinic conditions possibly  
155 expanded into a greater portion of the oceans at the onset of the Lau CIE as denoted by positive  
156 excursions in δ<sup>34</sup>S<sub>pyr</sub> and δ<sup>34</sup>S<sub>CAS</sub> (Fig. 2B, 3B). This onset of euxinia temporally coincides with the  
157 second wave of extinctions that affected planktic groups (i.e., ~75% loss in biodiversity of graptolites)  
158 and the rising limb of the CIE (Fig. 4A). Phytoplankton (i.e. acritarchs) actually increased in abundance  
159 immediately prior to and during the rising limb of the Lau CIE (Stricanne et al., 2006) as reducing  
160 conditions expanded, likely due to a lack of predation as zooplankton and larger marine taxa experienced  
161 earlier extinctions. Acritarchs finally declined with an associated ~95% drop in abundance during the  
162 peak of the CIE just before the global extent of euxinia reached a maximum, which is inferred by the  
163 rising limb nearing the peak of the δ<sup>34</sup>S<sub>CAS</sub> values.

164 In both the Gotland and Latvia δ<sup>34</sup>S records, peak excursion values post-date the corresponding  
165 peak δ<sup>13</sup>C values in the Lau CIE. The offset in these records suggests that organic carbon burial fueled  
166 high MSR rates, but may also be related to differences in oceanic residence times and/or continued pyrite  
167 burial post-CIE (e.g., Owens et al., 2013). The falling limb of the δ<sup>34</sup>S<sub>pyr</sub> record also lags the falling limb  
168 of the CIE, perhaps indicating the continued consumption of previously exported organic carbon after the  
169 termination of the burial event, which is corroborated by TI isotopes not returning to baseline values (cf.,  
170 Them et al., 2018). Regardless of the C-S offset and isotopic magnitudes, these large-magnitude S-isotope  
171 excursions that span ~ 1 Myr require a reduction in the marine sulfate reservoir, which was likely  
172 significantly lower than modern seawater (e.g., Gill et al., 2011).

## 173 174 **CONCLUSIONS**

175 The integrated paleontological and geochemical records suggest a stepwise extinction for the  
176 LKE was associated with the progressive expansion of reducing marine conditions. Increased anoxic and  
177 euxinic conditions likely shoaled from deeper shelf/slope areas to shallow platform settings during the  
178 Lau CIE. Our TI-isotope data provide detailed evidence for expanding marine deoxygenation in the  
179 interval that preceded the Lau CIE, coinciding with the initial phase of extinction. This was followed by  
180 global C- and S-isotope perturbations that coincide with continued marine extinction. This study  
181 highlights the role of oxygen depletion (i.e., non-sulfidic anoxia) near the onset of biotic change and  
182 provides a mechanism for the previously documented stepwise extinction event. The progressive  
183 expansion of oceanic anoxia leading to euxinia is a potential mechanism for extinction due to significant  
184 stress on marine ecosystems (Meyer and Kump, 2008), which might be similar to at least two Mesozoic  
185 OAEs. More broadly, this study indicates that global marine redox dynamics were a major driver in the  
186 evolution of the late Silurian biosphere, and potentially other Paleozoic biotic crises. The multi-proxy  
187 redox approach provides a more holistic global view of redox changes and supports recent evidence  
188 suggesting prevalent low oxygen conditions in the upper oceans of the Paleozoic (Lu et al., 2018).

## 189 190 **ACKNOWLEDGMENTS**

191 We thank N. Kozik, C. Richbourg, S. Newby, and E. Benayoun for assistance in sample  
192 processing and data collection; M. Calner for access to the Uddvide-1 core; four anonymous reviewers for  
193 their helpful reviews; and Judith Parrish for editorial handling of this manuscript. This research was  
194 funded by the National Science Foundation (EAR-1748635 to S.A.Y and J.D.O) and Estonian Research  
195 Council (PUT611 to D.K., O.H., and T.M.). This work was performed at the National High Magnetic  
196 Field Laboratory, which is supported by NSF Cooperative Agreement No. DMR-1644779 and the State  
197 of Florida.

## 198 199 **REFERENCES CITED**

200 Bond, D.P.G., and Grasby, S.E., 2017, On the causes of mass extinctions: Palaeogeography,  
201 Palaeoclimatology, Palaeoecology, v. 478, p. 3-29, doi: 10.1016/j.palaeo.2016.11.005.

202 Boyer, D.L., Owens, J.D., Lyons, T.W., and Droser, M.L., 2011, Joining forces: Combined biological and  
203 geochemical high-resolution palaeo-oxygen history in Devonian epeiric seas: *Palaeogeography,*  
204 *Palaeoclimatology, Palaeoecology*, v. 306, p. 134-146, doi: 10.1016/j.palaeo.2011.04.012.

205 Calner, M., 2005, A Late Silurian extinction event and anachronistic period: *Geology*, v. 33, no. 4, p. 305-  
206 308, doi: 10.1130/G21185.1.

207 Calner, M., 2008, Silurian global events — at the tipping point of climate change, *in* Elewa, A.M.T., ed.,  
208 *Mass extinctions: Berlin Heidelberg, Springer-Verlag*, p. 21-58.

209 Canfield, D.E., 1994, Factors influencing organic carbon preservation in marine sediments: *Chemical*  
210 *Geology*, v. 114, p. 315-329.

211 Cramer, B.D., Schmitz, M.D., Huff, W.D., and Bergström, S.M., 2015, High-precision U-Pb zircon age  
212 constraints on the duration of rapid biogeochemical events during the Ludlow Epoch (Silurian  
213 Period): *Journal of the Geological Society [London]*, v. 172, p. 157-160, doi: 10.1144/jgs2014-094.

214 Crampton, J.S., Cooper, R.A., Sadler, P.M., and Foote, M., 2016, Greenhouse—icehouse transition in the  
215 Late Ordovician marks a step change in extinction regime in the marine plankton: *Proceedings of the*  
216 *National Academy of Sciences*, v. 113, no. 6, p. 1498-1503, doi: 10.1073/pnas.1519092113.

217 Eriksson, M.J., and Calner, M., 2008, A sequence stratigraphical model for the Late Ludfordian (Silurian)  
218 of Gotland, Sweden: implications for timing between changes in sea level, palaeoecology, and the  
219 global carbon cycle: *Facies*, v. 54, p. 253-276, doi: 10.1007/s10347-007-0128-y.

220 Eriksson, M.E., Nilsson, E.K., and Jeppsson, L., 2009, Vertebrate extinctions and reorganizations during  
221 the Late Silurian Lau Event: *Geology*, v. 37, no. 8, p. 739-742, doi: 10.1130/G25709A.1.

222 Gill, B.C., Lyons, T.W., Young, S.A., Kump, L.R., Knoll, A.H., and Saltzman, M.R., 2011, Geochemical  
223 evidence for widespread euxinia in the Later Cambrian ocean: *Nature*, v. 469, p. 80-83, doi:  
224 10.1038/nature09700.

225 Jeppsson, L., 1998, Silurian oceanic events: summary of general characteristics, *in* Landing, E. and  
226 Johnson, M.E., ed., *Silurian cycles: linkages of dynamic stratigraphy with atmospheric, oceanic, and*  
227 *tectonic changes: James Hall Centennial Volume, New York State Museum Bulletin*, v. 491, p. 239-  
228 257.

229 Jeppsson, L., 2005, Conodont-based revisions of the Late Ludfordian on Gotland, Sweden: *Geologiska*  
230 *Föreningen (GFF)*, v. 127, p. 273-282, doi: 10.1080/11035890501274273.

231 Jeppsson, L., and Aldridge, R.J., 2000, Ludlow (late Silurian) oceanic episodes and events: *Journal of the*  
232 *Geological Society [London]*, v. 157, p. 1137-1148.

233 Kaljo, D., Kiipli, T., and Martma, T., 1997, Carbon isotope event markers through the Wenlock-Pridoli  
234 sequence at Ohesaare (Estonia) and Priekule (Latvia): *Palaeogeography, Palaeoclimatology,*  
235 *Palaeoecology*, v. 132, p. 211-223.

236 Koren', T.N., 1993, Main event levels in the evolution of the Ludlow graptolites: *Geological Correlation*,  
237 v. 1, p. 44-52.

238 Kump, L.R., Arthur, M.A., Patzowsky, M.E. Gibbs, M.T., Pinkus, D.S., Sheehan, P.M., 1999, A  
239 weathering hypothesis for glaciation at high atmospheric  $p\text{CO}_2$  during the late Ordovician:  
240 *Palaeogeography, Palaeoclimatology, Palaeoecology*, v. 152, p. 173-187.

241 Lu, W., Ridgwell, A., Thomas, E., Hardisty, D.S., Luo, G., Algeo, T.J., Saltzman, M.R., Gill, B.C., Shen,  
242 Y., Ling, H., Edwards, C.T., Whalen, M.T., Zhou, X., Gutches, K.M., Jin, L., Rickaby, R.E.M.,  
243 Jenkyns, H.C., Lyons, T.W., Lenton, T.M., Kump, L.R., and Lu, Z., 2018, Late inception of a  
244 resiliently oxygenated upper ocean: *Science*, v. 361, p. 174-177, doi: 10.1126/science.aar5372.

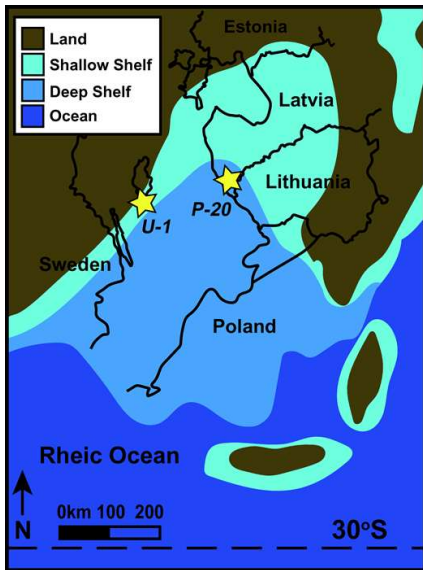
245 Manda, S., Štorch, P., Slavík, L., Fryda, J., Križ, J., and Tasáryová, A., 2012, The graptolite, conodont  
246 and sedimentary record through the late Ludlow Kozłowskii Event (Silurian) in the shale-dominated  
247 succession of Bohemia: *Geological Magazine*, v. 149, no. 3, p. 507-531, doi:  
248 10.1017/S0016756811000847.

249 Meyer, K.M., and Kump, L.R., 2008, Oceanic euxinia in earth history: Causes and consequences: *Annual*  
250 *Reviews of Earth and Planetary Science Letters*, v. 36, no. 1, p. 251-288, doi:  
251 10.1146/annurev.earth.36.031207.124256.

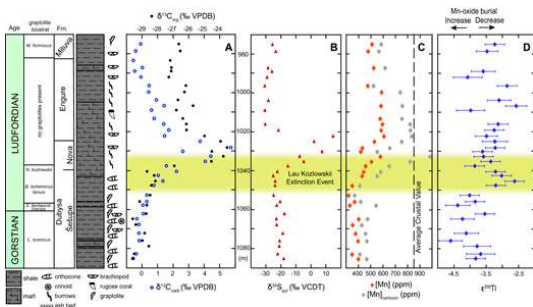
- 252 Munnecke, A., Samtleben, C., and Bickert, T., 2003, The Ireviken Event in the lower Silurian of Gotland,  
253 Sweden – relation to similar Palaeozoic and Proterozoic events: *Palaeogeography,*  
254 *Palaeoclimatology, Palaeoecology*, v. 195, p. 99-124, doi: 10.1016/S0031-0182(03)00304-3.  
255 Nielsen, S.G., Rehkämper, M., and Pritulak, J., 2017, Investigation and Application of Thallium Isotope  
256 Fractionation: *Reviews in Mineralogy & Geochemistry*, v. 82, p. 759-798, doi:  
257 10.2138/rmg.2017.82.18.  
258 Ostrander, C.M., Owens, J.D., and Nielsen, S.G., 2017, Constraining the rate of oceanic deoxygenation  
259 leading up to a Cretaceous Oceanic Anoxic Event (OAE-2: ~94 Ma), *Science Advances*, v. 3,  
260 e1701020.  
261 Owens, J.D., Gill, B.C., Jenkyns, H.C., Bates, S.M., Severmann, S., Kuypers, M.M.M., Woodfine, R.G.,  
262 and Lyons, T.W., 2013, Sulfur isotopes track the global extent and dynamics of euxinia during  
263 Cretaceous Oceanic Anoxic Event 2: *Proceedings of the National Academy of Sciences*, v. 110, p.  
264 18407-18412, doi: doi/10.1073/pnas.1305304110.  
265 Owens, J.D., Nielsen, S.G., Horner, T.J., Ostrander, C.M., and Peterson, L.C., 2017, Thallium-isotope  
266 compositions of euxinic sediments as a proxy for global manganese-oxide burial: *Geochimica et*  
267 *Cosmochimica Acta*, v. 213, p. 291-307, doi: 10.1016/j.gca.2017.06.041.  
268 Raven, M.R., Fike, D.A., Bradley, A.S., Gomes, M.L., Owens, J.D., and Webb, S.A., 2019, Paired  
269 organic matter and pyrite  $\delta^{34}\text{S}$  records reveal mechanisms of carbon, sulfur, and iron cycle disruption  
270 during Ocean Anoxic Event 2: *Earth and Planetary Science Letters*, v. 512, p. 27-38, doi:  
271 10.1016/j.epsl.2019.01.048.  
272 Saltzman, M.R., 2005, Phosphorus, nitrogen, and the redox evolution of the Paleozoic oceans: *Geology*,  
273 v. 33, 573-576, doi: 10.1130/G21535.1.  
274 Striccanne, L., Munnecke, A., and Pross, J., 2006, Assessing mechanisms of environmental change:  
275 Palynological signals across the Late Ludlow (Silurian) positive isotope excursion ( $\delta^{13}\text{C}$ ,  $\delta^{18}\text{O}$ ) on  
276 Gotland, Sweden: *Palaeogeography, Palaeoclimatology, Palaeoecology*, v. 230, p. 1-31, doi:  
277 10.1016/j.palaeo.2005.07.003.  
278 Talent, J.A., Mawson, R., Andrew, A.S., Hamilton, P.J., and Whitford, D.J., 1993, Middle Paleozoic  
279 extinction events: Faunal and isotopic data: *Palaeogeography, Palaeoclimatology, Palaeoecology*, v.  
280 104, p. 139-152.  
281 Them II, T.R., Gill, B.C., Caruthers, A.H., Gerhardt, A.M., Gröcke, D.R., Lyons, T.W., Marroquin, S.M.,  
282 Nielsen, S.G., Trabucho Alexandre, J.P., and Owens, J.D., 2018, Thallium isotopes reveal protracted  
283 anoxia during the Toarcian (Early Jurassic) associated with volcanism, carbon burial, and mass  
284 extinction: *Proceedings of the National Academy of Sciences*, p. 1-6, doi:  
285 10.1073/pnas.1803478115.  
286 Urbanek, A., 1993, Biotic crises in the history of the upper Silurian graptoloids: a paleobiological model:  
287 *Historical Biology*, v. 7, p. 29-50.  
288  
289

## 290 FIGURES

291

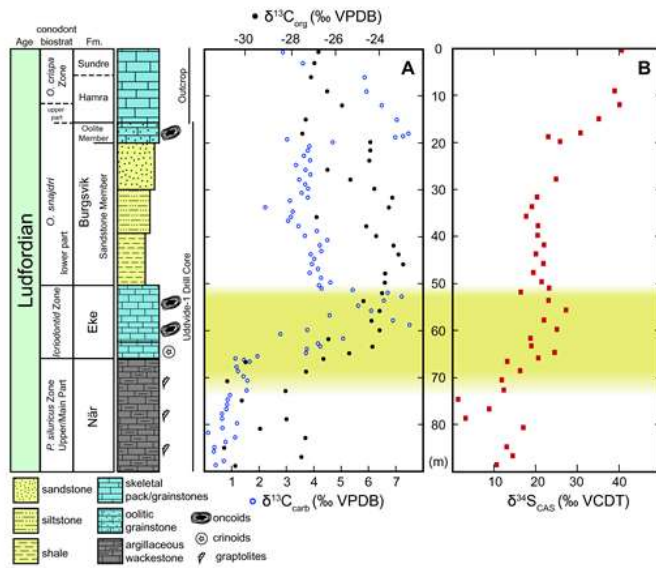


292  
 293 Figure 1. Paleogeographic reconstruction of the late Silurian Baltic Basin region (modified from Blakey  
 294 Europe Series, Silurian ca. 425 Ma; <https://www2.nau.edu/rcb7/>). Locations of the Gotland, Sweden  
 295 localities and the Latvian Priekule-20 drill core are marked by yellow stars. Detailed discussion of  
 296 correlation and biostratigraphy of the two localities can be found in the GSA Data Repository<sup>1</sup>.  
 297



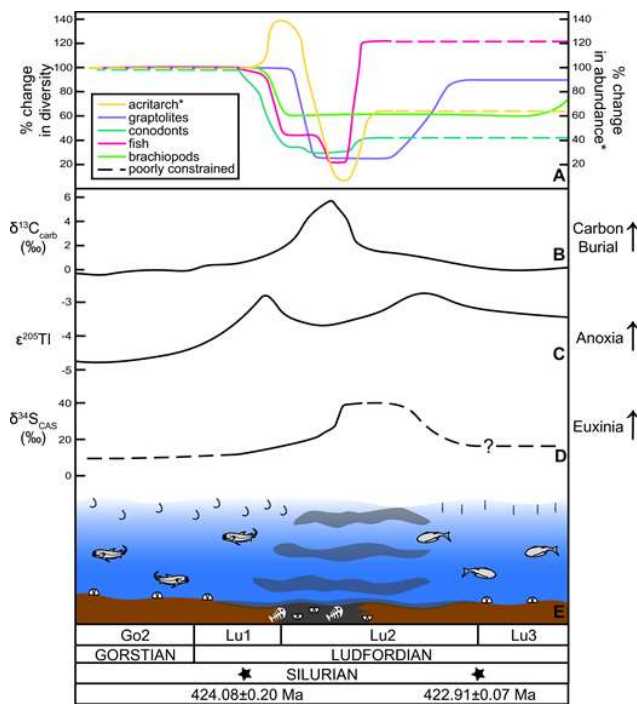
298  
 299 Figure 2. Geochemical data from the Priekule-20 drill core, near Priekule, Latvia. Graptolite biozones  
 300 after Kaljo et al. (1997). The Lau/Kozlowski extinction interval is shaded in yellow. Panel A: Carbonate  
 301 and organic carbon isotope data. Panel B: Pyrite sulfur isotope data. Panel C: Manganese concentration  
 302 data with the dashed line representing average crustal values. Panel D: Thallium isotope data plotted with  
 303  $2\sigma$  error bars.  
 304  
 305





306  
307  
308  
309  
310  
311  
312

Figure 3: Geochemical data from the Uddvide-1 drill core and nearby outcrops on Gotland, Sweden. Conodont biozones after Jeppsson (2005). The Lau/Kozłowski extinction interval is shaded in yellow. Panel A: Carbonate and organic carbon isotope data. Panel B: Carbonate associated sulfate (CAS) sulfur isotope data.



313  
314  
315  
316  
317  
318  
319

Figure 4: Summary figure of biotic, geochemical, and oceanographic events in the late Silurian that culminated in the LKE and Lau CIE. (A) Biotic data for acritarch (Stricanne et al., 2006), graptolite (Manda et al., 2012), conodont (Calner, 2008), fish (Eriksson et al., 2009), and brachiopod (Talent et al., 1993) extinctions. (B) Carbonate carbon isotope record. (C) Thallium isotope record indicating increased oceanic anoxia. (D) CAS sulfur isotope record suggesting increased euxinia; dashed portions are

320 expected, but currently unconstrained trends. € Depiction of the biotic and marine redox changes  
321 throughout the Gorstian and Ludfordian. Stars mark ~ positions of U-Pb zircon dates on K-bentonite ash  
322 beds from Podolia, Ukraine (Cramer et al., 2015). Construction of this figure detailed in the GSA Data  
323 Repository<sup>1</sup>.

324  
325 <sup>1</sup>GSA Data Repository item 201Xxxx, including analytical methods, geochemical data, and cross plots, is  
326 available online at [www.geosociety.org/pubs/ft20XX.htm](http://www.geosociety.org/pubs/ft20XX.htm), or on request from [editing@geosociety.org](mailto:editing@geosociety.org) or  
327 Documents Secretary, GSA, P.O. Box 9140, Boulder, CO 80301, USA.